

- 33 Pappas, T.C. *et al.* (1994) *Endocrine* 2, 813–822
- 34 Ramirez, V., Zheng, J. and Siddique, K. (1996) *Cell. Mol. Neurobiol.* 16, 175–198
- 35 Tischkau, S. and Ramirez, V. (1993) *Proc. Natl. Acad. Sci. U. S. A.* 90, 1285–1289
- 36 Orchinik, M., Murray, T.F. and Moore, F.L. (1991) *Science* 252, 1848–1851
- 37 Orchinik, M. *et al.* (1992) *Proc. Natl. Acad. Sci. U. S. A.* 89, 3830–3834
- 38 Minami, T. *et al.* (1990) *Brain Res.* 519, 301–307
- 39 Nabekura, J. *et al.* (1986) *Science* 233, 226–228
- 40 Mermelstein, P.G., Becker, J.B. and Surmeier, D.J. (1996) *J. Neurosci.* 16, 595–604
- 41 Mügge, A. *et al.* (1993) *Cardiovasc. Res.* 27, 1939–1942
- 42 French-Mullen, J.M.H. (1995) *J. Neurosci.* 15, 903–911
- 43 Gu, Q. and Moss, R.L. (1996) *J. Neurosci.* 16, 3620–3629
- 44 Wong, M. and Moss, R.L. (1991) *Brain Res.* 543, 148–152
- 45 White, R.E., Darkow, D.J. and Lang, J.L.F. (1995) *Circ. Res.* 77, 936–942
- 46 Dufy, B. *et al.* (1979) *Nature* 282, 855–857
- 47 Dubinsky, J.M. and Oxford, G.S. (1984) *J. Gen. Physiol.* 83, 309–339
- 48 Ritchie, A.K. (1987) *J. Physiol.* 385, 591–609
- 49 Matteson, D.R. and Armstrong, C.M. (1986) *J. Gen. Physiol.* 87, 161–182
- 50 Lingle, C.J., Sombati, S. and Freeman, M.E. (1986) *J. Neurosci.* 6, 2995–3005
- 51 Fomina, A.F. and Levitan, E.S. (1997) *Neuroscience* 78, 523–531
- 52 Lledo, P.-M. *et al.* (1990) *Endocrinology* 127, 990–1001
- 53 Drouva, S.V. *et al.* (1988) *Endocrinology* 123, 2762–2773
- 54 Attardi, B. *et al.* (1993) *Recept. Channels* 1, 287–293
- 55 Meza, U. *et al.* (1994) *J. Gen. Physiol.* 104, 19–38
- 56 Roberts, W., Jacobs, R. and Hudspeth, A. (1990) *J. Neurosci.* 10, 3664–3684
- 57 Monjaraz, E. *et al.* (1995) *Soc. Neurosci. Abstr.* 21, 1819
- 58 Fomina, A.F., Levitan, E.S. and Takimoto, K. (1996) *Neuroscience* 72, 857–862
- 59 Tashjian, A.H., Jr, Bancroft, F.C. and Levine, L. (1970) *J. Cell Biol.* 47, 61–70
- 60 Joubert-Bression, D. *et al.* (1990) in *Steroids and Neuronal Activity: Ciba Foundation Symposium 153* (Chadwick, D. and Widdows, K., ed.), pp. 156–171, Wiley
- 61 Lledo, P.-M. *et al.* (1992) *Neuron* 8, 455–463
- 62 Hopkins, C.D. (1974) *Z. Tierpsychol.* 35, 518–535
- 63 Mills, A.C. and Zakon, H.H. (1987) *J. Comp. Physiol.* 161, 417–430
- 64 Mills, A. and Zakon, H.H. (1991) *J. Neurosci.* 11, 2349–2361
- 65 Ferrari, M.B. and Zakon, H.H. (1993) *J. Comp. Physiol.* 173, 281–292
- 66 Dye, J. (1991) *J. Comp. Physiol.* 168, 521–532
- 67 Smith, G.T. and Zakon, H.H. (1997) *Soc. Neurosci. Abstr.* 23, 248
- 68 Condon, T.P., Dykshoorn-Bosch, M.A. and Kelly, M.J. (1988) *Biol. Reprod.* 38, 121–126
- 69 Kelly, M.J., Rønnekleiv, O.K. and Eskay, R.L. (1984) *Brain Res. Bull.* 12, 399–407
- 70 Kelly, M.J., Loose, M.D. and Rønnekleiv, O.K. (1992) *J. Neurosci.* 12, 2745–2780
- 71 Lagrange, A.H., Rønnekleiv, O.K. and Kelly, M.J. (1994) *J. Neurosci.* 14, 6196–6204
- 72 Lagrange, A.H., Rønnekleiv, O.K. and Kelly, M.J. (1995) *Endocrinology* 136, 2341–2344
- 73 Kelly, M.J., Lagrange, A.H. and Rønnekleiv, O.K. (1995) *Analgesia* 1, 494–497
- 74 Lagrange, A., Rønnekleiv, O. and Kelly, M. (1997) *Mol. Pharmacol.* 51, 605–612
- 75 Joëls, M., Hesen, W. and de Kloet, E.R. (1995) *J. Steroid Biochem. Mol. Biol.* 53, 315–323
- 76 Moss, R.L. (1997) *Recent Prog. Horm. Res.* 52, 33–69

Acknowledgements

The author thanks Bruce McEwen, Robert Moss, Ed Levitan, Martin Kelly, Aileen Ritchie, Kent Dunlap, G. Troy Smith and the two anonymous reviewers for helpful comments on the manuscript. The work from the author's lab has been supported by NIH grant number NS25513.

Extracellular space structure revealed by diffusion analysis

Charles Nicholson and Eva Syková

The structure of brain extracellular space resembles foam. Diffusing molecules execute random movements that cause their collision with membranes and affect their concentration distribution. By measuring this distribution, the volume fraction (α) and the tortuosity (λ) can be estimated. The volume fraction indicates the relative amount of extracellular space and tortuosity is a measure of hindrance of cellular obstructions. Diffusion measurements with molecules $<500 M_r$ show that $\alpha \approx 0.2$ and $\lambda \approx 1.6$, although some brain regions are anisotropic. Molecules $\geq 3000 M_r$ show more hindrance, but molecules of $70\,000 M_r$ can move through the extracellular space. During stimulation, and in pathophysiological states, α and λ change, for example in severe ischemia $\alpha = 0.04$ and $\lambda = 2.2$. These data support the feasibility of extrasynaptic or volume transmission in the extracellular space.

Trends Neurosci. (1998) 21, 207–215

THE NEURONS and glial cells of the brain are mingled together in an opaque mass with the consistency of soft jelly. The cells have complex shapes, yet remain distinct entities bounded by their membranes and separated from each other by an extracellular space (ECS). Despite the geometrical complexity of the ECS, its structure can be characterized by analyzing the way molecules diffuse within it¹.

The ECS has been likened to a foam² (Fig. 1). The width of the space varies and may contain 'lakes'^{3,4} (Fig. 1). Early attempts to use the electron microscope to measure the ECS found it to be almost non-

existent. Today, electron microscopy that preserves the ECS, radiotracer methods and the TMA⁺ method (tetramethylammonium method; Box 1), all agree that the average ECS volume is about 20% of the brain. Furthermore, radiotracer and TMA⁺ methods reveal new structural information about the ECS through the tortuosity factor, which will be described in detail in this review. Finally, diffusion analysis can provide data on the uptake, loss and binding of molecules.

The ECS exists for several reasons. It provides an extracellular microenvironment⁵, similar to that of cerebrospinal fluid, but with an additional matrix of

Charles Nicholson is at the Dept of Physiology and Neuroscience, New York University Medical Center, 550 First Avenue, New York, NY 10016, USA, and Eva Syková is at the Dept of Neuroscience, Institute of Experimental Medicine and 2nd Medical Faculty, Charles University, Videnská 1083, 142 20 Prague 4, Czech Republic.

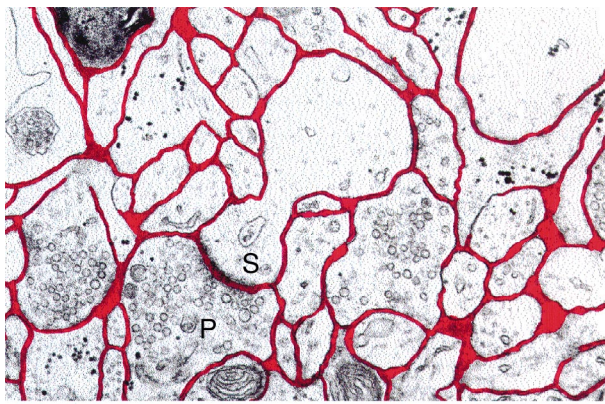


Fig. 1. Geometry of extracellular space. Electronmicrograph of small region of rat cortex with prominent dendritic spine (S) and presynaptic (P) terminal. The ECS is outlined in red. Note the foam-like structure, multiple connectivity, simple convex cell surfaces and presence of 'lakes' where the space widens. The ECS is probably reduced in width due to fixation procedure. Scale bar, 1 μm . Figure kindly provided by Dr C.B. Jaeger.

proteoglycans and glycosaminoglycans^{6,7}. The matrix composition varies with the cytoarchitectonics⁸, but we know little about its density and we lack reliable evidence that it affects diffusion. The ECS allows glucose to reach brain cells from the blood vessels. It provides a low-resistance path that completes the circuit

Box I. Diffusion measurements in the ECS

This box briefly outlines three diffusion methods that reveal structural information about the ECS. Values for the diffusion coefficients in water D , are given for some compounds in units of $10^{-6} \text{ cm}^2 \text{ s}^{-1}$. The apparent diffusion coefficient (ADC) D^* , can be calculated from $D^* = D/\lambda^2$ where λ is the tortuosity.

Radiotracers

Much of the pioneering work using the diffusion of radiotracers was carried out by Fenstermacher, Patlak and colleagues^{a-d} (Table 1). To determine the volume fraction, α and λ , a radiolabeled compound that remains in the ECS, such as [³H]inulin ($D = 2.5$; 37°C)^a, [¹⁴C]sucrose ($D = 7.1$; 37°C)^a or [¹⁴C]EDTA ($D = 7.0$; 37°C)^c was perfused into the appropriate subarachnoid space of an anesthetized animal for several hours, then the brain region quickly removed, frozen and sectioned. Brains were processed at intervals after commencing perfusion to obtain different profiles of radioactivity. Using a suitable solution to the diffusion equation, D^* could be calculated and compared with D measured in cylinders of agar. In some experiments, the loss or gain of substances across capillary walls was also estimated^b.

Radiotracer methods can characterize how many compounds distribute in the brain, including metabolites and chemotherapeutic compounds, but the method is limited because of the long perfusion periods and post-mortem processing involved. Radiotracer methods are still providing new data, for example on ischemic tissue^e and on the movement of nerve growth factor^f.

TMA⁺ method (real-time iontophoretic method)

This is the most widely used diffusion paradigm today. It originated in a study on K^+ diffusion by Lux and Neher^g that employed ion-selective microelectrodes (ISM). The original analysis was thwarted by the then-unrecognized issues of K^+ uptake and spatial buffering^h, but the technical approach was elaborated into the TMA⁺ (tetramethylammonium) method by Nicholson and Phillipsⁱ. The paradigm consists of the defined release of TMA⁺ (TEA⁺ may be used instead^j) from a source that approximates a point and its measurement at a known distance.

The TMA⁺ ($D = 13.0$; 37°C)ⁱ is usually released by iontophoresis from a micropipette, and distributes in the tissue according to Eqn 3 (Box 2). The local concentration of TMA⁺ is measured with an ISM (Ref. j) located about 100–200 μm from the release electrode (Fig. 3A). Appropriate calibration and curve fitting procedures are performed to fit Eqn 3 (Box 2), both in brain and in dilute gel, and the parameters α , λ and k' (where k' is uptake)

extracted. TMA⁺ (or TEA⁺) is used because it remains predominantly extracellular, and is small and does not alter physiological function at the concentrations usedⁱ; some anions can be used instead^j. The ISM can be substituted with a carbon-fiber microelectrode, permitting fast-scan cyclic voltammetry for measurement of the diffusion of electroactive substances such as dopamine^k. The small size of the source and measuring electrodes (tip diameter 2–12 μm) ensures that there is negligible edema or damage^l.

Integrative optical imaging (IOI)

It is of considerable interest to know how macromolecules permeate the ECS. The IOI-method was developed to determine D^* and λ for macromolecules tagged with fluorescent probes in living brain tissue using epifluorescence microscopy and quantitative image analysis^l (Fig. 4). By taking account of how the microscope images in-focus and out-of-focus points, the relative concentration of the diffusing cloud of molecules can be quantified^{lm}.

Studies have used dextrans^l with M_r of 3 kDa ($D = 2.33$; 34°C)^l, 10 kDa, 40 kDa and 70 kDa ($D = 0.38$; 34°C)^l. Further measurements employed lactalbuminⁿ with M_r of 14.4 kDa, ovalbuminⁿ with M_r of 45 kDa and bovine serum albumin (BSA)ⁿ with M_r of 66 kDa ($D = 0.83$; 34°C)ⁿ. Dextrans and albumins were delivered by a pressure-pulse method^l.

References

- a Levin, V.A., Fenstermacher, J.D. and Patlak, C.S. (1970) *Am. J. Physiol.* 219, 1528–1533
- b Patlak, C.S. and Fenstermacher, J.D. (1975) *Am. J. Physiol.* 229, 877–884
- c Kessler, J.A., Fenstermacher, J.D. and Owens, E.S. (1976) *Am. J. Physiol.* 230, 614–618
- d Fenstermacher, J.D. and Kaye, T. (1988) *Ann. New York Acad. Sci.* 531, 29–39
- e Newman, G.C. *et al.* (1995) in *Brain Slices in Basic and Clinical Research* (Schurr, A. and Rigor, B.M., eds), pp. 187–220, CRC
- f Krewson, C.E., Klarman, M.L. and Saltzman, W.M. (1995) *Brain Res.* 680, 196–206
- g Lux, H.D. and Neher, E. (1973) *Exp. Brain Res.* 17, 190–205
- h Nicholson, C., Phillips, J.M. and Gardner-Medwin, A.R. (1979) *Brain Res.* 169, 580–584
- i Nicholson, C. and Phillips, J.M. (1981) *J. Physiol.* 321, 225–257
- j Nicholson, C. (1993) *J. Neurosci. Meth.* 48, 199–213
- k Rice, M.E. and Nicholson, C. (1995) in *Voltammetric Methods in Brain Systems. Neuromethods 27* (Boulton, A.A., Baker, G.B. and Adams, R.N., eds), pp. 27–79, Humana
- l Nicholson, C. and Tao, L. (1993) *Biophys. J.* 65, 2277–2290
- m Tao, L. and Nicholson, C. (1995) *J. Microsc.* 178, 267–271
- n Tao, L. and Nicholson, C. (1996) *Neuroscience* 75, 839–847

TABLE 1. Comparison of different methods of measuring α and λ

Region	Animal	Substance	Method	α	λ	Refs
Cerebral cortex	Cat, dog, monkey	Sucrose, inulin	RT	0.19–0.20	1.39–1.44	15
Cerebral cortex	Rat	TMA ⁺	TMA ⁺	0.18–0.23	1.40–1.65	16–21
Cerebral cortex	Rat	Dextran 3–70 kDa	IOI	n/a	1.77–2.25	22
Cerebral cortex	Rat	Albumin 14.5–66 kDa	IOI	n/a	2.24–2.50	23
Corpus callosum	Rat	TMA ⁺	TMA ⁺	0.21–0.26	1.46, 1.70, 1.72 [#]	20,25
Hippocampus, CA1	Rat	TMA ⁺	TMA ⁺	0.12–0.14* 0.22	1.50–1.67* 1.50, 1.56, 1.80 [#]	21,24 25
Hippocampus, CA3	Rat	TMA ⁺	TMA ⁺	0.18–0.20* 0.22	1.57–1.83* 1.50, 1.62, 1.69 [#]	21,24 25
Caudate nucleus	Dog, rabbit rabbit, monkey	Sucrose, EDTA	RT	0.15–0.21	1.52–1.64	26,27
Caudate nucleus	Rat	TMA ⁺	TMA ⁺	0.21	1.54	44
Cerebellum, ML	Rat	TMA ⁺ , TEA ⁺ AsF ₆ ⁻ , α NS ⁻	TMA ⁺	0.18–0.26*	1.48–1.68*	1
Cerebellum, ML	Turtle	TMA ⁺	TMA ⁺	0.31	1.44, 1.95, 1.58 [#]	13
Cerebellum, GL	Turtle	TMA ⁺	TMA ⁺	0.21	1.77	13
Spinal cord	Monkey	Sucrose, EDTA	RT	0.14–0.18	2.0–2.1	29
Spinal cord, DH	Rat	TMA ⁺	TMA ⁺	0.2–0.22	1.54–1.62	30–33
Spinal cord, VH	Rat	TMA ⁺	TMA ⁺	0.23	1.46	30–33

[#]Three anisotropic values; * anisotropy was neglected in this study, although identified in subsequent work. Abbreviations: α , volume fraction; α NS⁻, α -naphthalene sulphonate; AsF₆⁻, hexafluoro arsenate; DH, dorsal horn; GL, granular layer; IOI, integrative optical imaging; λ , tortuosity; ML, molecular layer; n/a, not applicable; RT, radiotracer; TEA⁺, tetraethylammonium; TMA⁺, tetramethylammonium; VH, ventral horn.

for the transmembrane currents that generate action and synaptic potentials. Perhaps the most exciting role for the ECS, however, is as a communication channel⁹ between cells. This channel is distinct from classical synaptic transmission, and has been termed extrasynaptic or volume transmission^{10–12}.

Diffusion reveals structure

For many molecules, migration through the ECS is governed by diffusion. This observation can be turned around: the diffusion of ‘probe’ molecules can be used to reveal and quantify the structure of the ECS. Figure 2 shows how this comes about; Fig. 2A depicts several cellular profiles embedded in a bounded region of ECS and a red ‘+’ marking the site where molecules would be released. After release (Fig. 2B–2D), the molecules execute random ‘walks’ in the ECS. As the number of particles increases through Fig. 2B–2D, the structure of the ECS is revealed though the pattern of random walks.

Figure 2 shows that the process of diffusion is sensitive to ECS structure. This sensitivity can be captured by measuring the parameter that characterizes the diffusion process: the apparent diffusion coefficient (ADC). The ADC in the brain, often designated by D^* , can be compared to the diffusion coefficient (D) in water or a very dilute gel, through the tortuosity λ , a dimensionless number defined as $\lambda = (D/D^*)^{1/2}$. Since $D \geq D^*$, it follows that $\lambda \geq 1$. The tortuosity summarizes both the hindrance imposed by the cellular structures of the brain and the connectivity of the spaces. In principle, λ is sensitive to certain forms of uptake (Box 2) and the viscosity of the interstitial matrix; it is presently believed that such influences are small.

However, tortuosity is sensitive to molecular size and this reveals further information.

Tortuosity may also be anisotropic. This means that λ can have three distinct values: λ_x , λ_y and λ_z , each associated with a geometrical axis (i.e. that λ is a tensor). Diffusion anisotropy was first detected in the cerebellum¹³. Recently, anisotropy has become important in diffusion-weighted magnetic resonance imaging (DW-MRI) studies¹⁴. Diffusion analysis also reveals the relative volume in which the diffusing molecules are moving. This is the volume fraction of the ECS, denoted by:

$$\alpha = \text{volume of ECS} / \text{volume of tissue}$$

Volume fraction is also a dimensionless quantity and $\alpha \leq 1$.

Regional and comparative properties of the ECS

The most extensively studied ECS is that of the neocortex, but measurements have also been made on the corpus callosum, hippocampus, cerebellum, caudate nucleus and spinal cord. The diffusion properties have been measured with three major methods (described in Box 1): radiotracers, the TMA⁺ method (also known as the real-time iontophoretic method) and integrative optical imaging (IOI).

Cerebral cortex and corpus callosum

Radiotracer diffusion measurements¹⁵ have been made in the cat, dog and monkey (Table 1). More recently, the TMA⁺ method was employed in the anesthetized rat^{16,17}. The most detailed study¹⁸ determined a value for α of 0.19 (cortical layer II), which increased with depth to 0.23 (cortical layer VI), and λ of

Box 2. Microscopic and macroscopic diffusion in the ECS

On a microscopic scale, diffusion in the ECS can be described by the random walks of molecules as they collide frequently with water molecules and occasionally with obstructions such as cell membranes. With a suitable statistical treatment, the behavior of a large ensemble of random walks, or Brownian movement as it is also called, can be described by the equations of classical macroscopic diffusion^a; these equations originated from the work of Adolf Fick.

Diffusion measurements in the ECS involve distances of the order of 100 μm , and it is no longer relevant to talk of individual random walks of molecules. Fortunately, one can go seamlessly between the microscopic descriptions and the macroscopic; many of the underpinnings of this theoretical bridge are due to Albert Einstein^b.

The various things that can affect the substance as it distributes in the ECS are encapsulated in the macroscopic diffusion equation^{c,d}:

$$\frac{\partial C}{\partial t} = \frac{D}{\lambda^2} \nabla^2 C + \frac{Q}{\alpha} - \mathbf{v} \cdot \nabla C - \frac{f(C)}{\alpha} \quad (1)$$

The concentration (mM) is $C \equiv C(\mathbf{x}, t)$. Position (cm) is denoted by the vector \mathbf{x} (x, y, z in a Cartesian co-ordinate system or r, θ, φ in a spherical coordinate system) and time (s) denoted by t .

The structure of the tissue is introduced through two non-dimensional factors: the volume fraction and the tortuosity. Volume fraction (α) of the ECS is the ratio of the ECS volume to that of the total in a representative elementary tissue volume. Tortuosity (λ) is a measure of how diffusing molecules (path of travel shown in green, Fig. A) are hindered by cellular obstructions (Fig. A). Many early studies on the ECS focused on volume fraction, determined from the equilibrium distribution of radiotracers^e. Tortuosity appears explicitly in an early study on muscle^f and both

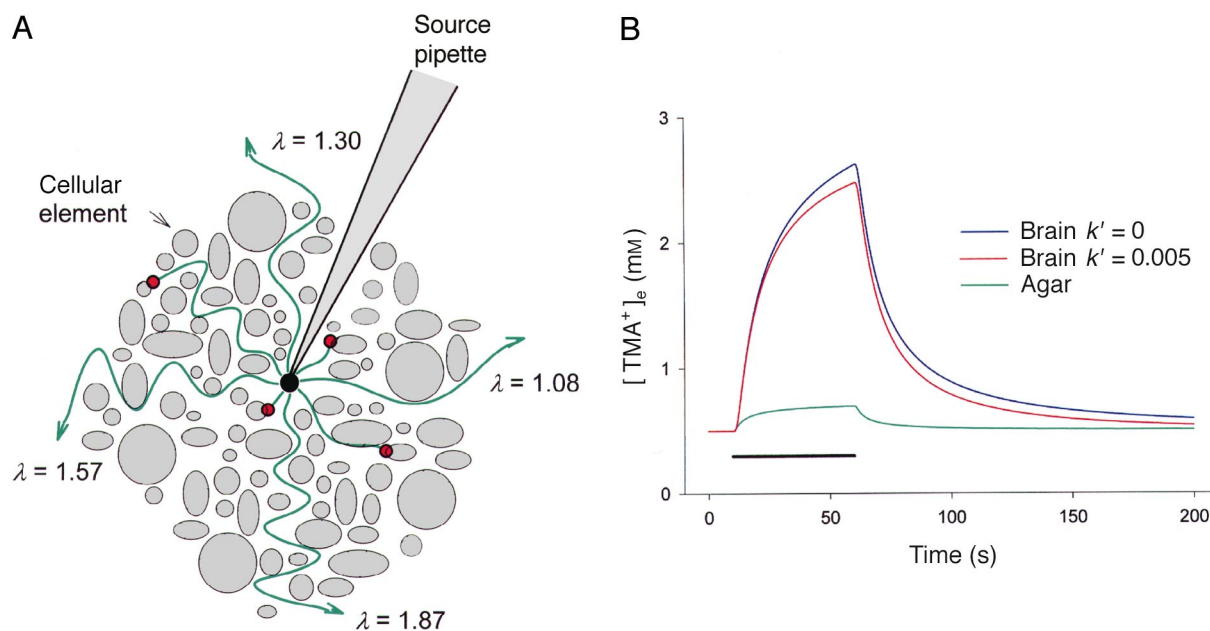


Fig. (A) Volume fraction, tortuosity and uptake. The concentration of a diffusing substance released from a microelectrode and confined to the ECS is modified by the volume fraction (α), tortuosity (λ) and uptake (k'). The volume fraction is represented here by the spaces between the cells, as a fraction of the whole volume, and the tortuosity is represented by the green lines emanating from the tip of the source electrode. The increase in length of the lines, relative to a straight line, is indicated on the figure (the calculation of tortuosity involves more complex averages over paths but this cartoon illustrates the idea). Additionally, diffusing molecules may be removed from the ECS at uptake sites (red dots) by a process represented by a suitable rate constant, k' (s^{-1}). **(B)** Theoretical diffusion curves illustrating effect of α , λ and k' . Curves computed from Eqn 3 using a spacing between iontophoretic source and ISM of 100 μm , a transport number (n) of 0.4 and a current of 100 nA for 50 s (indicated by the black bar). A background level of 0.5 mM TMA^+ in the agar and brain was assumed in the calculation. The green curve represents the result in dilute agar gel for which $\alpha = 1$, $\lambda = 1$ and $k' = 0$. The blue curve shows the result in typical brain tissue when $\alpha = 0.2$, $\lambda = 1.6$ and $k' = 0$. The red curve shows the same brain tissue, but now with $k' = 0.005 \text{ s}^{-1}$. It is evident that the combined effect of reduced volume fraction and increased tortuosity in brain, compared with a free medium, greatly increases the amplitude of the diffusion curve. The typical uptake usually seen in brain ($k' = 0.005 \text{ s}^{-1}$) makes a small but detectable difference; by routinely extracting the uptake contribution through appropriate non-linear curve fitting, the determination of α and λ is made more accurate.

1.51–1.65 in all layers in the adult rat. Other, more recent *in vivo* studies^{19,20} (Fig. 3A,B) confirmed these values, which are consistent with those obtained in cortical slices²¹. Values measured with radiotracers are similar but probably less accurate (Box 1). Tortuosities change when larger molecules are used to probe the ECS.

Studies with fluorescent dextrans²² revealed that λ increases from 1.77 to 2.25 as the M_r increases from 3 kDa to 70 kDa (Fig. 4; Table 1). Dextrans are loose aggregates

of long-chain sugar molecules. By contrast, albumins are compact proteins, but they too generate higher tortuosities²³ than TMA^+ (Table 1). One interpretation of these results is that the ECS is not uniform in size but has narrow regions that exclude the larger molecules, thus making them take a longer path as they diffuse. Alternatively, the size of the molecules might be comparable to the interstitial space leading to restricted diffusion³⁴. These data show that molecules as large as 70 kDa

volume fraction and tortuosity were employed in a paper on the cortex⁸. Tortuosity is a composite parameter that incorporates several geometric effects. If the ECS is viewed as a set of pores and the diameter of the molecule is comparable to the size of the pore, restricted diffusion^h could occur.

The term on the left of Eqn 1 represents the way that the concentration changes with time at any location. The first term on the right of the equal sign in Eqn 1 describes the contribution of diffusion itself. The free diffusion coefficient is D ($\text{cm}^2 \text{s}^{-1}$) and the ADC, $D^* = D/\lambda^2$. The symbol ∇^2 represents the second spatial derivative in the appropriate co-ordinate systemⁱ.

The second term is the source-term, $Q \equiv Q(\mathbf{x}, t)$ (mM s^{-1}), which can describe local iontophoretic^c, pressure pulse release of molecules^{d,i}, or local release of a substance from a cell.

The third term represents the contribution of flow, if present. Flow is defined by the vector \mathbf{v} (cm s^{-1}), and it forms a scalar product with the concentration gradient ∇C . Cserr and collaborators^k envisaged that molecular transport by bulk flow of fluid in the ECS was slow and took place in the restricted Virchow–Robin space adjacent to the brain capillaries. Bulk flow, when operative therefore, will have little influence on short-term and near-distance diffusion. Some evidence exists that peristaltic movements induced by vascular pulsation might disperse molecules within axon bundles^l.

The fourth term $f(C)$ (mM s^{-1}) represents uptake of material from the extracellular space, typically into cells, or degradation of the migrating substance by enzymatic attack or other kinetic processes^m. This term can also incorporate movement of substances across capillary wallsⁿ.

Presently, the most widely used diffusion paradigm is release of a substance from a point source and measurement of its concentration in the surrounding volume at various times and distances. Under these conditions, the diffusion is spherical, so the only spatial variable is r . It is usually assumed that bulk flow is zero and the uptake is driven by the concentration gradient across the cell membranes with the intracellular concentration of the substance being negligible. Then uptake can be defined by k' (s^{-1}) so that $f(C) = \alpha k' C$ in Eqn 1, which becomes:

$$\frac{\partial C}{\partial t} = \frac{D}{\lambda^2} \frac{1}{r^2} \frac{\partial}{\partial r} \left(r^2 \frac{\partial C}{\partial r} \right) + \frac{Q}{\alpha} - k' C \quad (2)$$

The appropriate solution for iontophoretic release (TMA⁺ method)^{c,d,m,o} is:

$$C(r,t) = \frac{Q}{8\pi D^* \alpha r} [h(r,t,\theta) - h(r,t,-\theta)]$$

and $h(r,t,\theta) =$

$$[g(r,t,\theta) - g(r,t-d,\theta)] \exp(r\theta)$$

where $D^* = D/\lambda^2$, $\theta = \sqrt{k'/D^*}$, (3)

$$g(r,t,\theta) = H(t) \operatorname{erfc} \left(r/2\sqrt{D^*t} + \theta\sqrt{D^*t} \right)$$

In Eqn 3, $H(t)$ is the Heaviside step function and $\operatorname{erfc}()$ is the complementary error function. For iontophoresis, the source term is $Q = In/F$, where I is the current (amps), n is the transport number for the substance and electrode, and F is Faraday's Electrochemical Equivalent. The duration of the source is d (s). Graphs of Eqn 3 are shown in Fig. B.

Equation 2 has been solved for when a substance is pressure-ejected from a source^{d,i,o}. Equations 1–3 have been extended^p to deal with anisotropy where λ is a tensor with three components, λ_x , λ_y and λ_z .

By using a non-linear curve fitting algorithm, such as the simplex, Eqn 3 can be fitted to experimental data and α , D^* and k' extracted. Obtaining α involves knowing n while λ can be calculated from D^* if D is known. Both n and D can be found by making diffusion measurements in a medium resembling the fluid in the ECS (actually NaCl solution in 0.3% agar or agarose to avoid thermal convection). In this medium, $\alpha = 1$, $\lambda = 1$ and $k' = 0$. The diffusion analysis algorithms for ion-selective microelectrodes, fast-scan voltammetry and both iontophoretic and pressure sources are incorporated in the program VOLTORO and a MATLAB program called Walter (both available for the PC from C. Nicholson).

This review focuses on the two structural parameters, α and λ ; values for k' can be found in many of the original papers, however. Typical values for TMA⁺ are $k' = 0.005 \text{ s}^{-1}$ in most brain regions (Fig. B illustrates effect of uptake). Note that certain types of fast reversible uptake (see ref. i, Chapter 14) are formally identical to an increase in λ . Finally, Eqs. 1–3 have been extended to describe the iontophoresis of dopamine with Michaelis–Menten uptake^m.

References

- a Berg, H.C. (1993) *Random Walks in Biology. Expanded Edition*, Princeton University Press
- b Einstein, A. (1956) *Investigations on the Theory of the Brownian Movement*, Dover
- c Nicholson, C. and Phillips, J.M. (1981) *J. Physiol.* 321, 225–257
- d Nicholson, C. (1992) *Can. J. Physiol. Pharmacol.* 70, S314–S322
- e Katzman, R. and Pappius, H.M. (1973) *Brain Electrolytes and Fluid Metabolism*, pp. 33–48, Williams and Wilkins
- f Harris, E.J. and Burn, G.P. (1948) *Trans. Faraday Soc.* 45, 508–528
- g McLennan, H. (1957) *Biochim. Biophys. Acta* 24, 1–8
- h Pappenheimer, J.R. (1953) *Physiol. Rev.* 33, 387–423
- i Crank, J. (1975) *The Mathematics of Diffusion* (2nd edn), Clarendon Press
- j Nicholson, C. (1985) *Brain Res.* 333, 325–329
- k Ichimura, T., Fraser, P.A. and Cserr, H.F. (1991) *Brain Res.* 545, 103–113
- l Bjelke, B. et al. (1995) *NeuroReport* 6, 1005–1009
- m Nicholson, C. (1995) *Biophys. J.* 68, 1699–1715
- n Patlak, C.S. and Fenstermacher, J.D. (1975) *Am. J. Physiol.* 229, 877–884
- o Nicholson, C. (1993) *J. Neurosci. Meth.* 48, 199–213
- p Rice, M.E., Okada, Y. and Nicholson, C. (1993) *J. Neurophysiol.* 70, 2035–2044

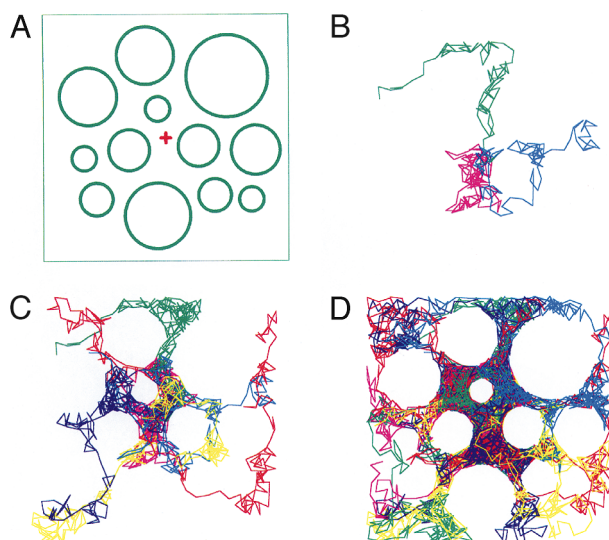
can diffuse through the ECS, even though their ADC (D/λ^2) is reduced fivefold compared with a free medium.

A study²⁰, using TMA⁺, of the corpus callosum (Fig. 3D) revealed that the tortuosity after myelination was anisotropic in this white matter region (Table 1). *Hippocampus, caudate nucleus and cerebellum*

Initial studies with the TMA⁺ method in the hippocampus^{21,24} revealed inhomogeneity, that is, α and λ had different values in different places (Table 1).

Recent studies²⁵ (Table 1), however, suggest that undetected anisotropy in the CA1 region could have led to an under-estimate of α in the original studies.

Radiotracer measurements in the caudate nucleus^{26,27} in dog, rabbit and monkey gave similar results to those obtained recently with the TMA⁺ method in slices of rat neostriatum (caudate nucleus; Table 1). The striatum is of special interest because of the possible role of dopamine as an extrasynaptic transmitter^{35,36}.



The cerebellum was the first brain region where the TMA⁺ method was employed^{1,37}. In addition, anionic probes were used¹ to look for any effect of negative charge on the diffusion properties of the extracellular matrix. No significant effect was seen in this early investigation, perhaps because the preponderance of Na⁺ (~150 mM) in the ECS screens negative charge.

The initial studies on the cerebellum¹ did not detect any anisotropy. More refined analysis¹³, however, showed that the molecular layer is anisotropic with $\lambda_x = 1.44$ along the parallel fibers, $\lambda_y = 1.95$ across the parallel fibers and in the plane of the pial surface, and $\lambda_z = 1.58$ in the vertical direction. The α of the molecular layer is 0.31, about 50% higher than that encountered in the cerebral cortex. The granular cell

layer, quite different structurally from the molecular layer, is isotropic (Table 1). Thus, the cerebellum exhibits both anisotropy and inhomogeneity. The anisotropy determined in the cerebellar molecular layer, the hippocampus and the corpus callosum will channel excess excitatory transmitters that spill over at the synapses³⁸ and other neuroactive substances, in specific directions¹³.

Spinal cord
Compared with recent TMA⁺ measurements^{30–33}, early radiotracer²⁹ measurements on the spinal cord of the monkey produced low values for α and high values for λ (Table 1). The TMA⁺ measurements show that the gray matter of the rat spinal cord has similar structural parameters to the cortex (Table 1). Anisotropic diffusion occurs, however, in spinal cord white matter (ventral funiculus)³³; as in the corpus callosum²⁰, this anisotropy only appears with myelination. In myelinated tissue, preferential diffusion of neuroactive substances and metabolites, therefore, might occur along the axons.

Spinal cord

The developing brain
Early studies used electron microscopy⁴ to address the fascinating issue of how the ECS changed its α as

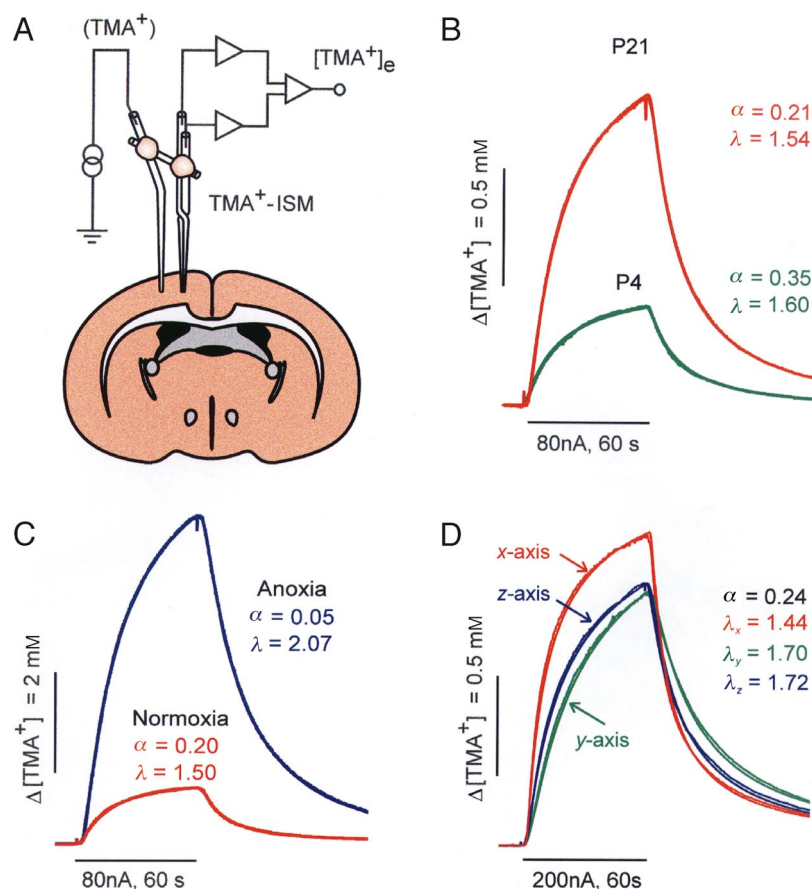


Fig. 3. Tetramethylammonium (TMA⁺) diffusion curves under different experimental conditions. (A) Schema of the experimental arrangement. A double-barreled, TMA⁺-selective microelectrode (TMA⁺-ISM) was glued to a bent iontophoresis microelectrode with a separation between electrode tips of 100–200 μm . (B–D) The ECS diffusion parameters α (volume fraction) and λ (tortuosity) are extracted by appropriate non-linear curve fitting. Experimental and theoretical curves (obtained using Eqn 3 in Box 2) are superimposed in each case; the concentration scale is linear. (B) Typical recordings obtained in rat cortex at postnatal days (P) four (shown in green) and 21 (shown in red). Values of α and λ are shown with each record. Note that the larger the curve, the smaller the value of α . (C) Typical recordings obtained in adult rat cortex (lamina V) during normoxia (red) and in the same animal at about 10 minutes after cardiac arrest (anoxia, shown in blue). (D) Representative records obtained in corpus callosum (CC) under anisotropic conditions, from diffusion measurements in three orthogonal axes [x (red), y (green) and z (blue)]. The x-axis lies along the axons; the y- and z-axes lie across the fibers in the CC. All recordings are from the same animal at P21 and were recorded with two microelectrode arrays. Recordings were first made with a microelectrode array in the x- and y-axes. The second microelectrode track was made with an array fixed in the y- and z-axes. The values in the y-axis were the same as those obtained with the first array (not shown). The shape and amplitude of the diffusion curves reflect the different apparent diffusion coefficients (ADCs) associated with each axis.

the animal developed. The results have been largely confirmed with TMA⁺ methods, which, in addition, have provided data on the λ .

In the cortex and corpus callosum of the newborn rat, α is about double (0.36–0.46) that of the adult^{18,20,39}, whereas λ in newborn rats is not significantly different from that in adults (Fig. 3B). The large ECS in the developing CNS might allow for the more effective diffusion of macromolecules, such as growth factors and cytokines. Diffusion might also be important in the developmental process itself^{12,40}.

Changes in the membrane currents of glial cells associated with myelination have been correlated with ECS diffusion parameters⁴¹. As a result of reduced α , membrane fluxes produce larger changes in extracellular K⁺ concentration in the mature, myelinated corpus callosum, compared with the newborn. The relationship between the ECS and membrane currents could also account for differences between currents measured in slices and those in tissue culture, where the ECS is effectively infinite. The size and geometry of the ECS may also influence the role of glial cells in spatial buffering of K⁺ (Ref. 41).

Diffusion parameters during stimulation and in pathological states

Given that α and λ exhibit approximately constant values throughout the normal brain, it is of interest to see how they change when the brain itself is altered.

Long-term changes in the parameters of the ECS accompany repetitive neuronal activity, nociceptive stimulation and pathological states^{12,30,41}. In the cat cortex, large changes in transmembrane fluxes of K⁺, Na⁺ and Cl⁻ are accompanied by the movement of water, cellular swelling and changes in α (Refs 42,43).
Osmotic stress

By combining TMA⁺ measurements with water content analysis, it is feasible to dissect the way water moves between the intracellular and extracellular compartments. In one study¹⁶, anesthetized rats were made hypernatremic, and the cortex lost water at the expense of the ECS, while regulatory mechanisms conserved cell volume. Another study²⁸ exposed the isolated turtle cerebellum to hypotonic medium, and α fell to 0.12, whereas in hypertonic medium α increased to as much as 0.60. Because total tissue volume hardly altered, the cells must have changed their volume. Tortuosity varied between 1.50 and 1.79 in these experiments²⁸.

Ischemia

During hypoxia and terminal anoxia *in vivo*, TMA⁺ measurements reveal that α in rat cortex^{17,19} (Fig. 3C) or spinal cord³¹ decreases to 0.04. It is remarkable that the volume fraction never falls below this value. In these experiments, λ increased to about 2.2, which seems to be the upper value that can be measured with a small molecule like TMA⁺ (but λ can be larger than 2.2 with macromolecules, even under normal conditions, Table 1). The time course of the changes in white matter is slower than in gray matter, and the time course in neonatal rats is about ten times slower than in adults¹⁹. This correlates with the well-known resistance of the immature CNS to anoxia. ECS diffusion parameters have also been studied in brain slices during hypoxia^{21,44}, where the changes in α and λ were slightly smaller than those *in vivo*. The changes in diffusion parameters during and after ischemia will enhance the accumulation of substances, contributing

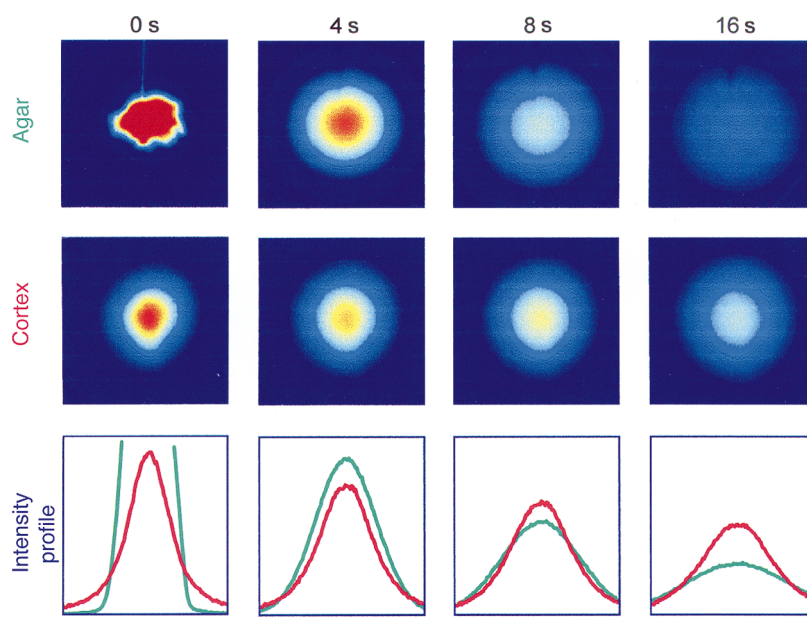


Fig. 4. Diffusion of 3 kDa dextran measured with IOI method. At time zero (0 s) a few nanoliters of 3 kDa dextran labeled with the fluorescent dye Texas Red were pressure ejected from a micropipette into either 0.3% agarose (agar) or a cortical slice. The cloud of dye molecules was viewed through an epifluorescent microscope and imaged with a cooled CCD camera²². Images are shown at four, eight and 16 s after the injection, with the dye concentration depicted in pseudo color (red highest concentration, blue lowest). The dextran diffuses away more quickly in the agarose (free medium) than in the cortex (hindered medium). The lowest panel shows concentration (intensity) profiles along a horizontal line through the center of the cloud of diffusing molecules; green profiles are from agar records, red from cortex. The profiles confirm the more rapid dispersion in the free medium compared with the hindered medium, and the characteristic bell-shaped curve of the concentration. Appropriate analysis of the curves enables D , D^* and λ to be obtained. Scale bar, 282 μm .

to brain damage and hindering the influx of metabolic substrates during any subsequent reperfusion.

DW-MRI and anoxia

DW-MRI (Ref. 45) is becoming a valuable tool for the diagnosis of brain anoxia. The ADC of water is reduced dramatically during anoxia and ischemia⁴⁶ but the mechanism of this reduction is still debated⁴⁷. A comparison⁴⁸ of the ADCs of TMA⁺ and water in rats 8–9 days of age during terminal anoxia has revealed very similar time courses, correlating with both a decrease in α and increase in λ . However, water can move freely across cellular membranes, whereas TMA⁺ stays predominantly in the ECS, and these experiments have not identified the mechanism that causes the changes of the ADC of water during anoxia.

Brain injury

Brain injury, with consequent neuronal death and astrogliosis, results in changes in ECS architecture. One model of brain injury is X-irradiation in the immature CNS, which is more sensitive to radiation than the adult⁴⁹.

In the cortex and corpus callosum of immature rats, X-irradiation results in radiation necrosis with typical early morphological changes in the tissue³⁹. X-irradiation at postnatal day (P) one not only blocked the expected decrease in α during postnatal development¹⁸, but caused α to increase to about 0.50 for several weeks after treatment³⁹. Tortuosity decreased 1–4 days after irradiation but 7–9 days later, the values were the same as control and 1–3 weeks after X-irradiation there was an unusual increase in λ . The rise in λ might be accounted for by diffusion barriers formed by new glial processes or changes in extracellular matrix expression.

Inflammatory and demyelinating diseases

Following intracerebral bacterial inoculation⁵⁰, acute inflammation and an increase in blood–brain barrier permeability in the abscess region occurred. There was a slightly larger α and slightly smaller λ than normal but without significant brain edema.

Dramatic changes in ECS diffusion parameters were found in the spinal cords of rats using a model of multiple sclerosis consisting of experimental autoimmune encephalomyelitis (EAE) induced by injection of myelin basic protein³². This resulted in paraparesis and damage to the blood–brain barrier accompanied by a transient increase in α to about 0.30 and a decrease in λ .

What diffusion has told us about the ECS

Molecules released from a source in the ECS perform countless random steps. In the process, they explore the intricate structure of the spaces that confine them. Two parameters, α and λ , give a summary of the exploration. Volume fraction (pore space or void fraction) and λ are well known in the study of porous media, which range from sandy beaches to chromatograph columns.

It is known (Table 1) that in most brain regions, α is about 0.2, whereas in homogeneous and isotropic brain regions, λ is about 1.5–1.6. This means that the ADC is reduced by 2.6 compared with water. The generality of these values are strikingly confirmed by diffusion measurements with the TMA⁺ method on the brains of cephalopod invertebrates⁵¹, which yield similar values to the vertebrates. During early development, α is considerably larger than in the adult.

The fact that 20% of the brain is ECS reflects the need for a significant brain extracellular microenvironment⁵. The magnitude of λ implies something about the structure of brain tissue. As often noted, the value of λ is close to $\pi/2$, the ratio of the path around a sphere to one through the center. This suggests that tortuosity is mainly determined by simple geometry and that the ECS is highly connected with generally convex, non-invaginated, cell surfaces. Furthermore, the viscosity of the ECS must be close to that in the CSF; this could imply that the density of the extracellular matrix is quite sparse. A general mathematical relationship between the random structure of the ECS and λ has yet to be formulated, although it can be given for aggregates of some regularly spaced cells.

The typical values for λ are based on the movement of molecules that are assumed sufficiently small to penetrate all regions of the ECS. When larger molecules are used ($M_r \geq 3000$), the measured λ increases and this suggests that some of the spaces in the brain might restrict the diffusion of macromolecules.

Stimulation of cells can lead to changes in α and λ , presumably because cells change their volume, indicating that the ECS is a dynamic entity. More extreme changes occur during simulated brain pathology. The resulting alterations in the ECS also influence the progression and recovery from the pathology itself. Osmotic or ischemic insults cause cellular swelling and consequent reduction in α and a rise in λ . Nevertheless, the spaces of the brain are never totally occluded. During longer-lasting injuries, such as X-irradiation and EAE, the behavior of the ECS is more complex. A persistent increase in λ , without a corresponding decrease in α was found during astrogliosis and in myelinated tissue. On both theoretical and

experimental grounds, α and λ seem to behave as independent variables. Long-term changes in λ might result from changes in the density of glial processes, or possibly from changes in the extracellular matrix, or both.

In addition to a structural description of the ECS, diffusion analysis also provides physiological information about the uptake or binding of molecules and their loss across the blood–brain barrier.

What are the implications of our new understanding of ECS structure for extrasynaptic or volume transmission? We know that a wide range of molecular sizes (at least up to 70 000 M_r) can migrate through the ECS, and from our knowledge of α and λ (Box 2) we can predict their diffusion behavior. This behavior can be modified by local inhomogeneity and by anisotropy in λ , which will tend to channel molecules in a particular direction. Furthermore, we have increasing evidence of selective ‘filtering’ of large molecules that might exclude them from certain regions of the ECS. Molecules enter the ECS either from the spillover of transmitter^{35,38} or by release from non-synaptic locations^{10,11,52}. For some molecules, such as dopamine, the extent of their migration can be determined by uptake or re-uptake^{35,53}. Finally, we know that the diffusion properties of the ECS can respond rapidly to neuronal activity and pathophysiology, and these effects could profoundly alter the way informational substances distribute⁵⁴. In conclusion, the new findings on the diffusion properties of the ECS further support the concept of volume transmission.

Selected references

- Nicholson, C. and Phillips, J.M. (1981) *J. Physiol.* 321, 225–257
- Kuffler, S.W. and Potter, D.D. (1964) *J. Neurophysiol.* 27, 290–320
- Van Harreveld, A., Crowell, J. and Malhotra, S.K. (1965) *J. Cell Biol.* 25, 117–137
- Bondareff, W. and Pysh, J.J. (1968) *Anat. Rec.* 160, 773–780
- Schmitt, F.O. and Samson, F.E. (1969) *Neurosci. Res. Prog. Bull.* 7, 277–417
- Margolis, R.K. and Margolis, R.U. (1993) *Experientia* 49, 429–446
- Ruoslahti, E. (1996) *Glycobiology* 6, 489–492
- Bignami, A. and Asher, R. (1993) *Int. J. Dev. Neurosci.* 10, 45–57
- Nicholson, C. (1979) in *The Neurosciences Fourth Study Program* (Schmitt, F.O. and Worden, F.G., eds), pp. 457–476, MIT Press
- Fuxe, K. and Agnati, L.F. (1991) *Volume Transmission in the Brain*, Raven Press
- Agnati, L.F. *et al.* (1995) *Neuroscience* 69, 711–726
- Syková, E. (1997) *The Neuroscientist* 3, 28–41
- Rice, M.E., Okada, Y. and Nicholson, C. (1993) *J. Neurophysiol.* 70, 2035–2044
- Le Bihan, D., Turner, R. and Douek, P. (1993) *NeuroReport* 4, 887–890
- Levin, V.A., Fenstermacher, J.D. and Patlak, C.S. (1970) *Am. J. Physiol.* 219, 1528–1533
- Cserr, H.F. *et al.* (1991) *J. Physiol.* 442, 277–295
- Lundbæk, J.A. and Hansen, A.J. (1992) *Acta Physiol. Scand.* 146, 473–484
- Lehmenkühler, A. *et al.* (1993) *Neuroscience* 55, 339–351
- Voříšek, I. and Syková, E. (1997) *J. Cereb. Blood Flow Metab.* 17, 191–203
- Voříšek, I. and Syková, E. (1997) *J. Neurophysiol.* 78, 912–919
- Pérez-Pinzón, M.A., Tao, L. and Nicholson, C. (1995) *J. Neurophysiol.* 74, 565–573
- Nicholson, C. and Tao, L. (1993) *Biophys. J.* 65, 2277–2290
- Tao, L. and Nicholson, C. (1996) *Neurosci. J.* 75, 839–847
- McBain, C.J., Traynelis, S.F. and Dingledine, R. (1990) *Science* 249, 674–677
- Mazel, Šimonová, Z. and Syková, E. *NeuroReport* (in press)
- Patlak, C.S. and Fenstermacher, J.D. (1975) *Am. J. Physiol.* 229, 877–884
- Fenstermacher, J.D. and Kaye, T. (1988) *Ann. New York Acad. Sci.* 531, 29–39
- Krizaj, D. *et al.* (1996) *J. Physiol.* 492, 887–896
- Kessler, J.A., Fenstermacher, J.D. and Owens, E.S. (1976) *Am. J. Physiol.* 230, 614–618
- Svoboda, J. and Syková, E. (1991) *Brain Res.* 560, 216–224
- Syková, E. *et al.* (1994) *J. Cereb. Blood Flow Metab.* 14, 301–311
- Šimonová, Z. *et al.* (1996) *Physiol. Res.* 45, 11–22

Acknowledgement

We are grateful to Dr Margaret Rice for critically reading the manuscript.

Supported by grants: NS 28642 and NS 34115, from the US National Institutes of Health (CN) and GACR No. 309/96/0884, 307/96/K226, 309/97/K048 and IGA M2 3423-3 and VS 96-130 from Czech Grant Agencies (ES).

- 33 Prokopová, S., Vargová, L. and Syková, E. (1997) *NeuroReport* 8, 3527–3532
- 34 Pappenheimer, J.R. (1953) *Physiol. Rev.* 33, 387–423
- 35 Garris, P.A. and Wightman, R.M. (1994) *J. Neurosci.* 14, 442–450
- 36 Rice, M.E. and Nicholson, C. (1995) in *Voltammetric Methods in Brain Systems. Neuromethods 27* (Boulton, A.A., Baker, G.B. and Adams, R.N., eds), pp. 27–79, Humana
- 37 Nicholson, C., Phillips, J.M. and Gardner-Medwin, A.R. (1979) *Brain Res.* 169, 580–584
- 38 Barbour, B. and Häusser, M. (1997) *Trends Neurosci.* 20, 377–384
- 39 Syková, E. *et al.* (1996) *Neuroscience* 70, 597–612
- 40 Kennedy, T.E. *et al.* (1994) *Cell* 78, 425–435
- 41 Chvátal, A. *et al.* (1997) *J. Neurosci. Res.* 49, 98–106
- 42 Dietzel, I. *et al.* (1980) *Exp. Brain Res.* 40, 432–439
- 43 Dietzel, I. *et al.* (1982) *Exp. Brain Res.* 46, 73–84
- 44 Rice, M.E. and Nicholson, C. (1991) *J. Neurophysiol.* 65, 264–272
- 45 Le Bihan, D., ed. (1995) *Diffusion and Perfusion Magnetic Resonance Imaging. Applications to Functional MRI*, Raven Press
- 46 Moseley, M.E. *et al.* (1990) *Magn. Reson. Med.* 14, 330–346
- 47 Szafer, A. *et al.* (1995) *NMR Biomed.* 8, 289–296
- 48 Van der Toorn, A. *et al.* (1996) *Magn. Reson. Med.* 36, 52–60
- 49 Gutin, P.H., Leibel, S.A. and Sheline, G.E., eds (1991) *Radiation Injury to the Nervous System*, Raven Press
- 50 Lo, W.D. *et al.* (1993) *J. Neurol. Sci.* 118, 188–193
- 51 Nicholson, C. *et al.* (1993) in *Cephalopod Neurobiology* (Abbott, N.J., Williamson, R. and Maddock, L., eds), pp. 383–397, Oxford University Press
- 52 Rice, M.E. *et al.* (1994) *Exp. Brain Res.* 100, 395–406
- 53 Nicholson, C. (1995) *Biophys. J.* 68, 1699–1715
- 54 Schmitt, F.O. (1984) *Neuroscience* 13, 991–1001

Orphanin FQ/nociceptin: a role in pain and analgesia, but so much more

Tristan Darland, Mary M. Heinricher and David K. Grandy

The publication of the δ opioid receptor sequence led to the cloning of three homologous receptors: the μ and κ opioid receptors, and a novel opioid-like orphan receptor. The orphan receptor's endogenous ligand, a 17-amino-acid peptide that resembles dynorphin, was named 'orphanin FQ' and 'nociceptin' (OFQ/N₁₋₁₇). The OFQ/N₁₋₁₇ receptor is expressed widely in the nervous system, and it is becoming clear that the peptide is likely to participate in a broad range of physiological and behavioral functions. At the cellular level, OFQ/N₁₋₁₇ has much in common with the classical opioids; however, functional studies are now revealing distinct actions of this peptide. Identified only two years ago, OFQ/N₁₋₁₇ has already attracted a great deal of attention. The number and diversity of papers focused on OFQ/N₁₋₁₇ at the recent meeting of the Society for Neuroscience augur an exciting future for this new peptide.

Trends Neurosci. (1998) 21, 215–221

MORE THAN 30 years of research has established that opioids activate three distinct classes of G protein-coupled receptor: μ , κ and δ . However, additional receptor subtypes such as μ_1 and μ_2 , and κ_1 , κ_2 and κ_3 (Ref. 1) were subsequently proposed to explain some of the more puzzling aspects of opioid pharmacology. As a consequence, cloning of the δ opioid receptor by Evans *et al.*² and Kieffer *et al.*³ sparked an intense international effort to clone the remaining members of this potentially large gene family.

It was, therefore, something of a surprise that instead of the expected multitude of opioid receptors, the products of only four distinct genes have so far been cloned. Three of these encode the classic δ , μ and κ opioid receptors^{4,5}. Interestingly, although the fourth encodes a receptor (variously known as LC132, ORL1, XOR, ROR-C and KOR3) that was originally identified because of its extensive nucleotide sequence homology with the δ receptor^{6,7} (see Ref. 8 for a recent review), this receptor does not bind opioid ligands with high affinity. It came to be known as the 'opioid-like orphan receptor', and the race to identify its endogenous ligand was on.

The endogenous ligand for the opioid-like orphan receptor: orphanin FQ/nociceptin₁₋₁₇

At the 1995 meeting of the International Narcotics Research Conference in St Andrews, Scotland, J.C.

Meunier reported the isolation of a 17-amino acid peptide from rat brain that decreased forskolin-stimulated cAMP production *in vitro*. A paper terming this peptide 'nociceptin' was subsequently published by Meunier *et al.*⁹ A peptide of identical sequence, isolated from pig brain, was reported simultaneously by Reinscheid *et al.*¹⁰ who named it orphanin FQ (OFQ; Fig. 1)^{11,12}. For the purposes of this article, the peptide will be referred to as 'orphanin FQ/nociceptin' (OFQ/N). The studies conducted by Reinscheid *et al.*¹⁰ demonstrated that a monoiodinated, tyrosine-substituted analog of OFQ/N₁₋₁₇ has nanomolar affinity for the opioid-like orphan receptor, and couples it to the inhibition of forskolin-stimulated cAMP production in a naloxone-insensitive manner.

Several groups have subsequently modified the sequence of the OFQ/N₁₋₁₇ peptide. In one study, Reinscheid *et al.*¹³ performed a systematic scanning mutagenesis survey and determined that, although residues in the amino-terminal portion of the peptide are important, the entire sequence is required for high affinity binding to, and activation of, the rat OFQ/N receptor expressed in Chinese hamster ovary (CHO) cells. In another study, Butour *et al.*¹⁴ reported similar findings using membranes prepared from CHO cells that express the human receptor whereas Shimohigashi *et al.*¹⁵ found that several synthetic derivatives of OFQ/N₁₋₁₇ display

Tristan Darland is at the Dept of Cell and Developmental Biology, Oregon Health Sciences University, Portland, OR, USA, Mary M. Heinricher is at the Depts of Neurosurgery and of Physiology and Pharmacology, OHSU, Portland, OR, USA, and David K. Grandy is at the Dept of Physiology and Pharmacology, OHSU, Portland, OR, USA.